Salinity sensor based on polyimide-coated photonic crystal fiber

Chuang Wu,[1,3] Bai-Ou Guan,[4] Chao Lu,[1] and Hwa-Yaw Tam[2,*]

[1]*Photonics Research Centre, Department of Electronic and Information Engineering, The Hong Kong Polytechnic University, Kowloon, Hong Kong, China*
[2]*Photonics Research Centre, Department of Electrical Engineering, The Hong Kong Polytechnic University, Kowloon, Hong Kong, China*
[3]*School of Physics and Optoelectronic Engineering, Dalian University of Technology, Dalian 116024, China*
[4]*Institute of Photonics Technology, Jinan University, Guangzhou 510632, China*
*eehytam@polyu.edu.hk

Abstract: We proposed and experimentally demonstrated a highly sensitive salinity sensor using a polyimide-coated Hi-Bi photonic crystal fiber Sagnac interferometer based on the coating swelling induced radial pressure. This is the first time to exploit fiber coating induced pressure effect for salinity sensing. The achieved salinity sensitivity is 0.742 nm/(mol/L), which is 45 times more sensitive than that of a polyimide-coated fiber Bragg grating. A bare fiber Bragg grating is incorporated into the fiber loop for temperature compensation.

References and links

1. P. St. J. Russell, "Photonic-crystal fibers," J. Lightwave Technol. **24**(12), 4729–4749 (2006).
2. B. J. Eggleton, C. Kerbage, P. S. Westbrook, R. S. Windeler, and A. Hale, "Microstructured optical fiber devices," Opt. Express **9**(13), 698–713 (2001).
3. O. Frazão, J. L. Santos, F. M. Araújo, and L. A. Ferreira, "Optical sensing with photonic crystal fibers," Laser Photonics Rev. **2**(6), 449–459 (2008).
4. H. Y. Choi, M. J. Kim, and B. H. Lee, "All-fiber Mach-Zehnder type interferometers formed in photonic crystal fiber," Opt. Express **15**(9), 5711–5720 (2007).
5. J. Villatoro, V. P. Minkovich, V. Pruneri, and G. Badenes, "Simple all-microstructured-optical-fiber interferometer built via fusion splicing," Opt. Express **15**(4), 1491–1496 (2007).
6. W. W. Qian, C. L. Zhao, S. L. He, X. Y. Dong, S. Q. Zhang, Z. X. Zhang, S. Z. Jin, J. T. Guo, and H. F. Wei, "High-sensitivity temperature sensor based on an alcohol-filled photonic crystal fiber loop mirror," Opt. Lett. **36**(9), 1548–1550 (2011).
7. V. P. Minkovich, J. Villatoro, D. Monzón-Hernández, S. Calixto, A. Sotsky, and L. Sotskaya, "Holey fiber tapers with resonance transmission for high-resolution refractive index sensing," Opt. Express **13**(19), 7609–7614 (2005).
8. B. Gu, M. J. Yin, A. P. Zhang, J. W. Qian, and S. L. He, "Low-cost high-performance fiber-optic pH sensor based on thin-core fiber modal interferometer," Opt. Express **17**(25), 22296–22302 (2009).
9. B. Gu, M. J. Yin, A. P. Zhang, J. W. Qian, and S. L. He, "Optical fiber relative humidity sensor based on FBG incorporated thin-core fiber modal interferometer," Opt. Express **19**(5), 4140–4146 (2011).
10. Q. Wu, Y. Semenova, J. Mathew, P. Wang, and G. Farrell, "Humidity sensor based on a single-mode hetero-core fiber structure," Opt. Lett. **36**(10), 1752–1754 (2011).
11. J. Cong, X. M. Zhang, K. S. Chen, and J. Xu, "Fiber optic Bragg grating sensor based on hydrogels for measuring salinity," Sens. Actuators B Chem. **87**(3), 487–490 (2002).
12. L. Q. Men, P. Lu, and Q. Y. Chen, "A multiplexed fiber Bragg grating sensor for simultaneous salinity and temperature measurement," J. Appl. Phys. **103**(5), 053107 (2008).
13. N. Díaz-Herrera, O. Esteban, M. C. Navarrete, M. Le Haitre, and A. González-Cano, "*In situ* salinity measurements in seawater with a fibre-optic probe," Meas. Sci. Technol. **17**(8), 2227–2232 (2006).
14. D. J. Gentleman and K. S. Booksh, "Determining salinity using a multimode fiber optic surface plasmon resonance dip-probe," Talanta **68**(3), 504–515 (2006).
15. R. Falate, O. Frazão, G. Rego, J. L. Fabris, and J. L. Santos, "Refractometric sensor based on a phase-shifted long-period fiber grating," Appl. Opt. **45**(21), 5066–5072 (2006).
16. G. R. C. Possetti, R. C. Kamikawachi, C. L. Prevedello, M. Muller, and J. L. Fabris, "Salinity measurement in water environment with a long period grating based interferometer," Meas. Sci. Technol. **20**(3), 034003 (2009).
17. D. A. Pereira, O. Frazão, and J. L. Santos, "Fiber Bragg grating sensing system for simultaneous measurement of salinity and temperature," Opt. Eng. **43**(2), 299–304 (2004).

18. L. V. Nguyen, M. Vasiliev, and K. Alameh, "Three-Wave Fiber Fabry–Pérot Interferometer for Simultaneous Measurement of Temperature and Water Salinity of Seawater," IEEE Photon. Technol. Lett. **23**(7), 450–452 (2011).
19. C. L. Zhao, X. Yang, C. Lu, W. Jin, and M. S. Demokan, "Temperature-insensitive interferometer using a highly birefringent photonic crystal fiber loop mirror," IEEE Photon. Technol. Lett. **16**(11), 2535–2537 (2004).
20. D. H. Kim and J. U. Kang, "Sagnac loop interferometer based on polarization maintaining photonic crystal fiber with reduced temperature sensitivity," Opt. Express **12**(19), 4490–4495 (2004).
21. G. Statkiewicz, T. Martynkien, and W. Urbańczyk, "Measurements of modal birefringence and polarimetric sensitivity of the birefringent holey fiber to hydrostatic pressure and strain," Opt. Commun. **241**(4-6), 339–348 (2004).
22. X. Y. Dong, H. Y. Tam, and P. Shum, "Temperature-insensitive strain sensor with polarization-maintaining photonic crystal fiber based Sagnac interferometer," Appl. Phys. Lett. **90**(15), 151113 (2007).
23. H. Y. Fu, H. Y. Tam, L. Y. Shao, X. Y. Dong, P. K. A. Wai, C. Lu, and S. K. Khijwania, "Pressure sensor realized with polarization-maintaining photonic crystal fiber-based Sagnac interferometer," Appl. Opt. **47**(15), 2835–2839 (2008).
24. H. Y. Fu, C. Wu, M. L. Tse, L. Zhang, K. C. Cheng, H. Y. Tam, B.-O. Guan, and C. Lu, "High pressure sensor based on photonic crystal fiber for downhole application," Appl. Opt. **49**(14), 2639–2643 (2010).
25. H. Y. Fu, A. C. L. Wong, P. A. Childs, H. Y. Tam, Y. B. Liao, C. Lu, and P. K. A. Wai, "Multiplexing of polarization-maintaining photonic crystal fiber based Sagnac interferometric sensors," Opt. Express **17**(21), 18501–18512 (2009).
26. M. L. V. Tse, H. Y. Tam, L. B. Fu, B. K. Thomas, L. Dong, C. Lu, and P. K. A. Wai, "Fusion splicing holey fibers and single-mode fibers: A simple method to reduce loss and increase strength," IEEE Photon. Technol. Lett. **21**(3), 164–166 (2009).
27. M. G. Xu, L. Reekie, Y. T. Chow, and J. P. Dakin, "Optical in-fiber grating high pressure sensor," Electron. Lett. **29**(4), 398–399 (1993).
28. A. D. Kersey, M. A. Davis, H. J. Patrick, M. LeBlanc, K. P. Koo, C. G. Askins, M. A. Putnam, and E. J. Friebele, "Fiber grating sensors," J. Lightwave Technol. **15**(8), 1442–1463 (1997).
29. C. Wu, H. Y. Fu, H. Y. Au, B. O. Guan, and H. Y. Tam, "High-sensitivity salinity sensor realized with photonic crystal fiber Sagnac interferometer," Proc. SPIE **7753**, 77531B (2011).

1. Introduction

Tremendous research effort has been invested in the study of photonic crystal fibers (PCFs) in the last decade [1]. PCFs exhibit structural flexibility and new light guiding mechanism that distinguishes them from conventional fibers in many aspects. Benefiting from these novel properties, various fiber-optic devices [2] have been developed based on PCFs particularly in fiber sensors [3]. In addition to the unique features reported in [1–3], PCFs also possess the advantages of conventional optical fibers in sensing applications such as EMI immunity, compact size, corrosion resistance, light weight, multiplexing capability, etc. Optical fiber sensors are also attractive for *in situ* monitoring of different physical, chemical, and biological parameters, e.g., strain [4, 5], temperature [6], refractive index [7], pH [8], relative humidity [9, 10], and water salinity [11–18]. Salinity sensors play an important role in manufacturing process control and protection of ecosystems. Fiber optic salinity sensors have been reported based on salinity sensitive hydrogel/polyimide-coated fiber Bragg gratings (FBG) [11, 12], surface Plasmon resonance effect [13, 14], and refractive index detection with long-period fiber gratings [15, 16], etched FBG [17], and femtosecond laser micro-machined Fabry–Pérot interferometer [18] to derive salinity response. However, these salinity sensors have relatively low sensitivity and/or exhibit large temperature cross sensitivity which degrades the sensor performance.

In this paper, a novel fiber optic salinity sensor based on polyimide-coated polarization-maintaining photonic crystal fiber (PM-PCF) Sagnac interferometer is presented. The PM-PCF has been investigated for different sensing applications [19–25], in which the two most interesting achievements are temperature insensitivity and ultrahigh pressure-sensitivity [23]. By exploiting the high pressure-sensitivity and the coating swelling induced radial pressure, a high salinity sensitivity of 0.742 nm/(mol/L) is achieved, which is 45 times more sensitive than FBG-based salinity sensors reported in [12]. Although the PM-PCF itself is insensitive to temperature, the coating's thermal expansion causes a temperature sensitivity of −0.0149 nm/°C. Thus a bare FBG was incorporated into the fiber loop for temperature compensation. This paper reports some important improvements over our earlier work [29].

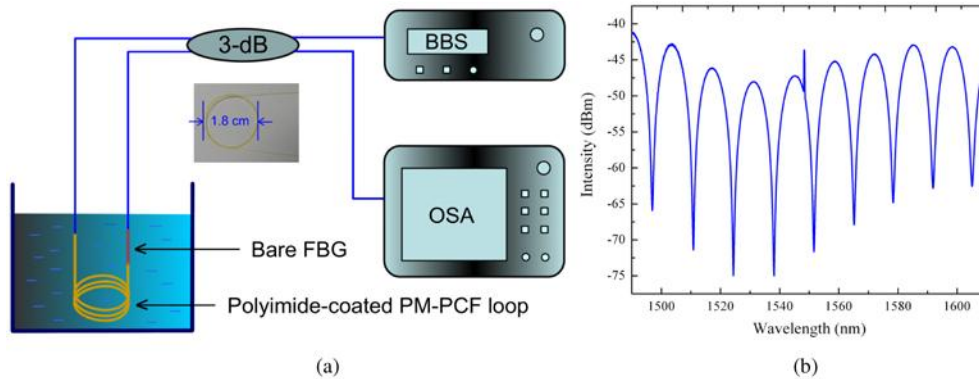## 2. Experimental setup and operation principle

Fig. 1. (a) Schematic of the water salinity measurement setup. The inset shows the photograph of the polyimide-coated PM-PCF salinity sensor coiled into 1.8-cm diameter loops. BBS: broadband light source; OSA: optical spectrum analyzer. (b) The output spectrum of the sensor head: a Sagnac interferometer combined with a fiber Bragg grating.

Figure 1 (a) illustrates the experimental setup for water salinity measurement. The light source used in the experiment is a broadband light source which is a superluminescent light-emitting diode (SLED) centered at 1550 nm. The salinity sensor consists of a 3-dB coupler, a 20.8-cm long polyimide-coated PM-PCF and an FBG arranged within the fiber loop. The PM-PCF was coiled into a small circle with a diameter of 1.8 cm. The PM-PCF used in the experiments is a commercially available fiber (PM-1550-01, NKT Photonics) and has a high birefringence with beat length less than 4 mm at 1550 nm. Furthermore, it has very low temperature sensitivity and an ultra low bending loss [23]. These merits make it ideal for making compact sensor probe. The PM-PCF can be easily spliced to single-mode fiber, achieving both low splicing loss and good mechanical strength [26]. The total splicing loss was ~3 dB for the two splicing points. Note that the relatively small splicing loss ensures that the Bragg reflection of the FBG can be observed regardless of the interference fringe's shift. Figure 1 (b) shows the output spectrum of the sensor observed by an optical spectrum analyzer. The interference pattern has an intensity contrast of over 25 dB and a period of 13.52 nm, and the FBG reflection wavelength peak is at 1548.38 nm.

An automated polyimide (PI) recoater (Vytran PTR-200-PRL) was used to recoat the PM-PCF. We stripped off the acrylate coating of the PM-PCF and then recoated the fiber with PI. The coating thickness is about 18 μm. By using the automated recoater, a very smooth coating with uniform coating thickness can be easily achieved. To ensure the stability of the Sagnac interferometer for salinity measurement, we coiled the PM-PCF to make the sensing head compact and secured it on a steel rod. Then the sensor head was submerged in water inside a water tank as shown in Fig. 1 (a).

The swelling property of the polyimide coating is related to the water salinity and ambient temperature. With an increase in water salinity, the PI coating shrinks [12] and produces a compressive radial pressure as well as a negative axial strain on the fiber. For a PI-coated FBG, the pressure effect is neglectable since the pressure sensitivity of a FBG is only −3.05 pm/MPa [27]; the negative axial strain effect accounts for the salinity sensitivity and causes the Bragg wavelength blue shift as reported in [12]. However, the pressure sensitivity of a PM-PCF Sagnac interferometer has been demonstrated as high as 3.24 nm/MPa [23], which is 1000 times higher than that of an FBG. A small increase in pressure can lead to a large wavelength shift in a PM-PCF Sagnac interferometer. On the other hand, the PM-PCF Sagnac interferometer has a fairly low strain sensitivity of 0.23 pm/με [22], which is even smaller than that of an FBG (1.2 pm/με [28]). As a result, the radial pressure effect accounts for the salinity sensitivity of PI-coated PM-PCF Sagnac interferometer and will cause the spectrum red shift since the pressure sensitivity has a positive sign. With an increase in temperature, the

PI coating expands, and this counteracts some of salinity-induced pressure, i.e., the pressure decreases and thus causes the spectrum blue shift. The bare FBG in the fiber loop is only sensitive to temperature. So temperature compensation can be achieved using the following matrix [12]:

$$\begin{vmatrix} \Delta T \\ \Delta S \end{vmatrix} = \frac{1}{K_{S,Sagnac} \cdot K_{T,FBG}} \begin{vmatrix} K_{S,Sagnac} & 0 \\ -K_{T,Sagnac} & K_{T,FBG} \end{vmatrix} \begin{vmatrix} \Delta\lambda_{FBG} \\ \Delta\lambda_{Sagnac} \end{vmatrix},$$ (1)

where $K_{S,Sagnac}$ and $K_{T,Sagnac}$ are salinity and temperature sensitivities of the PI-coated Sagnac interferometer, respectively; $K_{T,FBG}$ is the temperature sensitivity of the FBG.

3. Experimental results and discussion
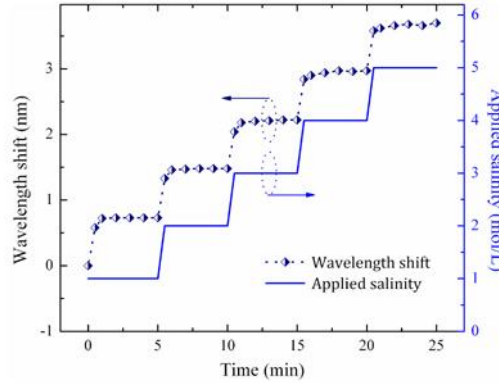
3.1 Salinity response

Fig. 2. Dynamic response of the sensor to change in water salinity.

The water tank was first filled with 100-mL of pure water. Saturated NaCl solution with a concentration of 5.5 mol/L was added to the water to vary the salinity of the solution. Solid NaCl was not used as it would take longer time to dissolve in water and would affect the measurement accuracy when characterizing the time response of the sensor. Figure 2 shows the time response of the Sagnac wavelength shift at different salinities. A fast response time of about one minute was measured for the sensor. Figure 3 (a) shows the output spectra of the sensor at different salinities. The FBG reflection wavelength peak remains unchanged when the salinity was varied from 0 mol/L to 5 mol/L, whereas the Sagnac interference minimum wavelengths shifted by about 3.736 nm. Figure 3 (b) shows the wavelength shift as a function of water salinity. Three measurements were carried out to verify its repeatability. Through a linear fitting, the salinity sensitivity of the PM-PCF Sagnac interferometer was found to be 0.742, 0.738 and 0.743 nm/M (M means mol/L for water salinity) for the three measurements, respectively, and that of the FBG is zero. This sensitivity is 45 times higher than the previous reported value of 0.0165 nm/M, which was based on a PI-coated FBG [12]. In addition, it is at least 6 times more sensitive than that of hydrogel-coated FBG [11]. One advantage of PI over hydrogel is its high temperature sustainability (up to 300 °C) and this makes our proposed salinity sensor suitable for harsh environment application. What's more, PI is widely used as fiber coating to enhance the mechanical strength of optical fibers for protection, which is crucial in engineering. Thus mature PI-recoater is commercially available, and such setup enables us fabricate PI coating with ease. However, for fabrication of hydrogel coating, it usually involves specially designed holder and UV-curing equipment, which is much more complex than the former.
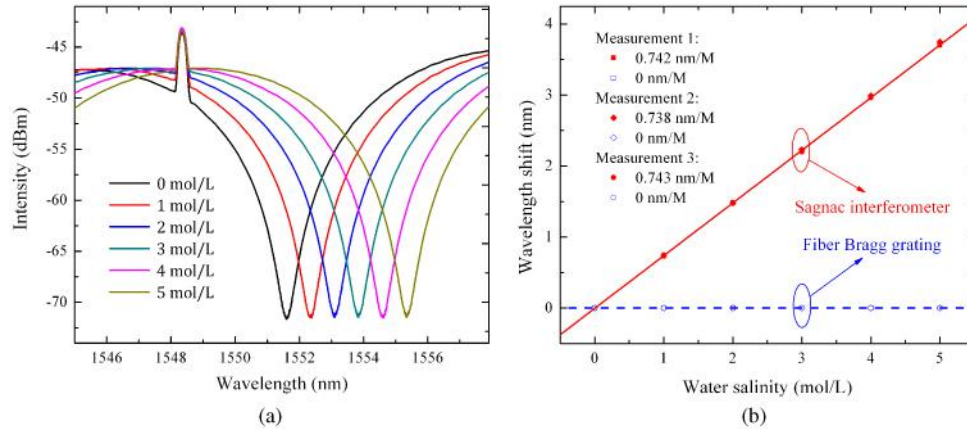
Fig. 3. (a) Spectra at different salinities for measurement 1. (b) Wavelength shift as a function of water salinity for three measurements.

To find out how salinity sensitivity depends on the length (*L*) of PM-PCF, we consider the pressure sensitivity of a PM-PCF Sagnac interferometer. Refs [23] and [24] demonstrated that such interferometers with different *L*s showed similar pressure sensitivities. It can be expected that the PI-coated interferometers with different *L*s will also have similar salinity sensitivities since they are based on pressure effect of the coating. Note that the 20.8-cm PM-PCF we used is just an example, and the length of 20.8-cm is not a necessary value. The salinity sensitivity can be further improved by using a thicker PI coating at the expense of longer response time. A thicker coating will induce larger pressure and hence result in higher salinity sensitivity. However it will take longer time to response to ambient environmental change. Limited by the recoater, we can only fabricate PI coating with a maximum thickness of 18 μm.
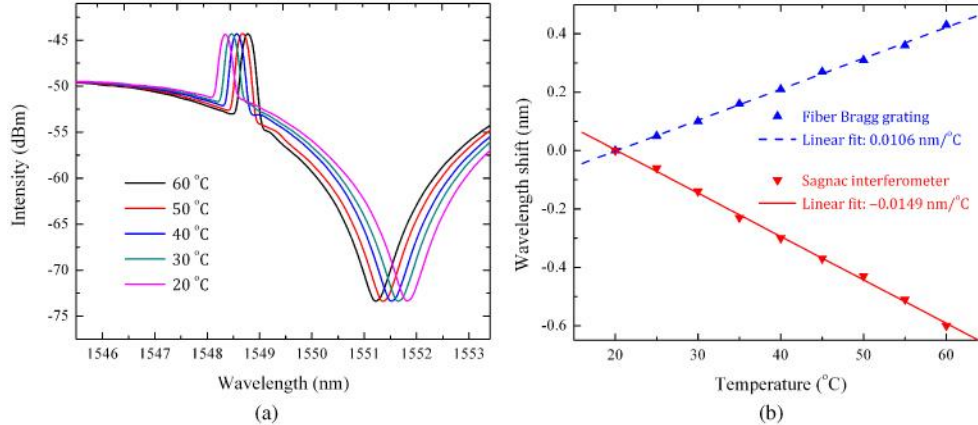
3.2 Temperature response and compensation

Fig. 4. (a) Spectra at different temperatures. (b) Wavelength shift as a function of temperature.

Temperature cross sensitivity of sensors is a big concern for real application since temperature fluctuation is inevitable in most applications and therefore affect the accuracy of the sensors. The sensor head was placed inside a hot water bath to investigate its temperature response. Data were collected when the temperature of the water bath was falling from 60 °C to 20 °C during the cooling-down process with steps of 5 °C. As shown in Fig. 4 (a) and (b), the FBG red shifts with a sensitivity of 0.0106 nm/°C, whereas the Sagnac interferometer blue shifts with a sensitivity of −0.0149 nm/°C which is at the same order of the grating based salinity

sensors [11, 12]. Hence, our sensor exhibits lower cross-sensitivity to temperature since it has much higher salinity sensitivity than that of the grating based sensors.

Using the salinity and temperature sensitivities obtained above, and substituting them to Eq. (1), temperature compensation can be performed using Eq. (2).

$$\begin{bmatrix} \Delta T \\ \Delta S \end{bmatrix} = \frac{1}{0.742 \times 0.0106} \begin{bmatrix} 0.742 & 0 \\ 0.0149 & 0.0106 \end{bmatrix} \begin{bmatrix} \Delta\lambda_{FBG} \\ \Delta\lambda_{Sagnac} \end{bmatrix}, \tag{2}$$

where $\Delta\lambda_{FBG}$ and $\Delta\lambda_{Sagnac}$ are in nm, ΔT and ΔS are obtained in °C and mol/L, respectively. Based on this equation, temperature and salinity can be simultaneously determined. To verify whether such a temperature compensation scheme works, we measured the water salinity at different temperatures using our sensor and the results are shown in Fig. 5. The standard deviations for the two measurements are 0.026 and 0.027 mol/L, which mainly come from the inaccuracy during data collection and the limitation of the OSA resolution (0.02 nm). The resolution of salinity measurement can be calculated as: 0.02 nm / 0.742 nm/(mol/L) = 0.027 mol/L, which is comparable with above error values.
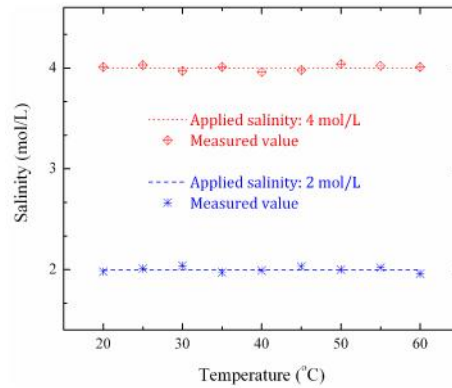

Fig. 5. Demonstration of temperature compensation for salinity measurements.

4. Summary

In conclusion, we report a highly sensitive fiber-optic salinity sensor using a PI-coated PM-PCF Sagnac interferometer by exploiting the high pressure-sensitivity of the PM-PCF Sagnac interferometer and the coating swelling induced radial pressure effect on the fiber. This is the first time to exploit fiber coating induced pressure effect for salinity sensing. The achieved salinity sensitivity is 45 times higher than that of a PI-coated FBG. In addition, temperature compensation was successfully implemented by incorporating a bare FBG into the fiber loop. This fiber-optic salinity sensor features high sensitivity, compact size, ease for fabrication, and good thermal stability.